

# Bayesian Projections of the Amur and Selenga River Runoff Changes in the 21st Century Based on CMIP6 Model Ensemble Simulations

A. S. Lipavskii<sup>a, b</sup>, A. V. Eliseev<sup>a, c, d, e\*</sup>, and I. I. Mokhov<sup>a, c, f</sup>

<sup>a</sup>Lomonosov Moscow State University, GSP-1, Leninskie Gory, Moscow, 119991 Russia

<sup>b</sup>Shirshov Institute of Oceanology, Russian Academy of Sciences, Nakhimovskii pr. 36,  
Moscow, 117997 Russia

<sup>c</sup>Obukhov Institute of Atmospheric Physics, Russian Academy of Sciences, Pyzhevskii per. 3,  
Moscow, 119017 Russia

<sup>d</sup>Kazan (Volga Region) Federal University, ul. Kremlevskaya 18, Kazan, 420008 Russia

<sup>e</sup>Institute of Applied Physics, Russian Academy of Sciences, GSP-120, ul. Ul'yanova 46,  
Nizhny Novgorod, 603950 Russia

<sup>f</sup>Moscow Institute of Physics and Technology, Institutskii per. 9, Dolgoprudny,  
Moscow oblast, 141700 Russia

\*e-mail: eliseev.alexey.v@gmail.com

Received September 27, 2021

Revised December 20, 2021

Accepted January 10, 2022

**Abstract**—The analysis is carried out for changes in runoff of the Amur and Selenga rivers in the 21st century according to the CMIP6 (Coupled Model Intercomparison Project, Phase 6) climate model ensemble simulations using the Bayesian approach versus stream gage data on annual runoff and GPCP-2.3 dataset on annual precipitation over catchments on different timescales. For both catchments, significant intermodel differences are associated with the projections of multiyear mean runoff and interannual variability. The intermodel distribution of Bayesian weights indicates a high role of uncertainty related to initial conditions for model simulations. There is a positive trend in total runoff in the Amur River basin in the 21st century under all analyzed anthropogenic forcing scenarios. For total runoff of the Selenga River, there are no trends in the 21st century for all analyzed scenarios. No significant trends for the Amur and Selenga surface runoff were revealed for all algorithms for considering Bayesian weights and all anthropogenic forcing scenarios. At the same time, significant interdecadal variations in the interannual variability of runoff were found.

**DOI:** 10.3103/S1068373922050065

**Keywords:** River runoff, Amur River, Selenga River, CMIP6 climate model ensemble, Bayesian weights

## 1. INTRODUCTION

River runoff (water discharge in a river channel) is the major component both of hydrological processes and regional climate as a whole [1–3, 5, 7, 9, 10, 13, 17–19, 21, 22, 25, 28, 37, 39–42, 49]. In case of relatively small changes in soil moisture and in the absence of artificial structures on a river (dams, reservoirs) on interannual and longer timescales, river runoff is determined by the integral difference between precipitation and evapotranspiration over the river catchment. Extremely low and extremely high values of river runoff on the mentioned timescales are associated with extreme climatic variations manifested in the respective variations in the hydrological cycle [9, 13, 21, 48, 49]. In particular, with the projected continuation of global warming in the 21st century along with further changes in runoff on a secular scale [5, 17, 21, 47, 49], a significant change in the probability of extreme hydrological events with reduced and extremely high runoff is expected [13, 21, 48].

There are long time series of river runoff measurements (see, for example, <https://portal.grdc.bafg.de/applications/>), and the analysis of climatic variations on interdecadal and secular scales is possible for rivers with large catchments. This fundamentally distinguishes river runoff from a number of other significant climatic variables, including hydrological ones.

Due to the problem of global climate change, projections of future changes in river runoff are needed (for example, [13, 15]). Such projections are possible only using global climate models [5, 15–17, 21, 32, 47, 49] and regional hydrological models [45]. Regional hydrological models have high spatial resolution as compared to the Earth system models, they can take into account local hydrological processes and, therefore, are characterized by higher accuracy. At the same time, hydrological models utilize the Earth system model output as boundary conditions and do not consider hydrological feedback with the state of the atmosphere. Climate is characterized by internal natural variability, model output depends on initial conditions, uncertainty of model projections should be taken into account [30, 35]. External forcing, both anthropogenic and natural, can change according to different scenarios (pathways). Uncertainty is also associated with the model features: with the consideration or non-consideration of various processes, parameterizations of subgrid-scale processes, program code details (these features are referred to so called structural uncertainty), as well as with specific values of model coefficients (“control parameters,” i.e., parametric uncertainty).

Uncertainty in the estimates of future changes in the climatic characteristics associated with specifying initial conditions, as a rule, is considerably reduced as a result of ensemble averaging. In its turn, the ensemble averaging does not obligatorily reduce a corresponding spread related to the model features. Nevertheless, mutually uncorrelated components of intermodel variations in a specific variable (and, hence, a part of uncertainty of projections of its possible future changes) can be excluded when computing ensemble statistics of simulation results for the ensembles of climate models [6, 8, 11, 33, 34, 43]. The Bayesian approach with individual model weighting and subsequent analysis of different variants of weights for assessing the sensitivity of results to such choice was taken to implement the averaging.

It is interesting to compare the results of simulations with the ensemble of the Earth system models and the ensemble of hydrological models. According to [4], when using hydrological model simulations, the normals of annual runoff are close to zero under the RCP 2.6 and RCP 4.5 scenarios and reach  $-5\dots-7\%$  by the end of the 21st century under the RCP 8.5 scenario. At the same time, for the Selenga River, a decrease in the normal of annual runoff is projected almost for the entire 21st century for all scenarios used [12].

The objective of this paper is to analyze changes in runoff of the Amur and Selenga rivers in the 21st century according to the simulations with the CMIP6 (Coupled Model Intercomparison Project, Phase 6, climate model ensemble (<https://esgf-node.llnl.gov/projects/cmip6/>)). It is essential that the size of the Amur and Selenga catchments ( $1.9 \cdot 10^6$  and  $\sim 0.5 \cdot 10^6$  km<sup>2</sup>, respectively) is much greater than the typical size of a horizontal cell of modern climate models ( $\sim 10^3$  km<sup>2</sup>). The Amur River with annual runoff of  $\sim 350$  km<sup>3</sup>/year [27] is among the most water-abundant rivers of the world. The Selenga River with annual runoff of  $\sim 30$  km<sup>3</sup>/year [9, 20] is the major tributary of the largest freshwater reservoir (Lake Baikal). A distinctive feature of the Amur and Selenga rivers is that the formation of precipitation in their catchments is associated both with cyclonic processes and with monsoon activity [9, 11, 13, 15, 20].

## 2. DATA AND METHODS

The changes in surface and total runoff  $R$  (the variables  $mrrros$  and  $mrrro$ , respectively) for the Amur and Selenga rivers were analyzed using the Bayesian averaging based on the simulations with the ensemble of CMIP-6 latest-generation climate models for “historical” numerical experiments and SSPs (Shared Socio-economic Pathways) 1-2.6, 2-4.5, 5-8.5 for 1979–2100 (see Table 1). Surface runoff is determined in the models as runoff from the simulated soil layer (with a thickness of several centimeters). Total runoff in the models from a unit area of soil almost (with an accuracy to the accumulation of moisture in soil) closes (relative to the difference between precipitation and evapotranspiration) the hydrological balance of the catchment on an annual and longer timescales. However, the latter case does not take into account the filling or emptying of underground water reservoirs, as well as (in some models) the water discharge for irrigation. In view of the latter, both variables were used to analyze model river runoff.

The models were selected from the general ensemble, for which both variables (precipitation and runoff) were synchronously presented for the “historical” numerical experiment and at least one of the mentioned SSPs. In the presence of simulations with different initial conditions for the same model, only one of them was analyzed (11 in the CMIP6 archive).

**Table 1.** The CMIP6 ensemble models whose simulations were used for the analysis

Number	Model in the CMIP6	Atmosphere model	Land surface model	Horizontal resolution, degree
1	ACCESS-CM2	MetUM-HadGEM3-GA7.1	CABLE2.5	1.25 1.875
2	BCC-CSM2-MR	BCC_AGCM3_MR	BCC_AVIM2	(S) 1.125 1.125
3	CanESM5	CanAM5	CLASS3.6/CTEM1.2	(S) 2.813 2.813
4	CESM2-WACCM	WACCM6	CLM5	1.25 0.938
5	CMCC-CM2-SR5	CAM5.3	CLM4.5-BGC	1.25 0.938
6	E3SM-1-1	EAM-1.1	ELM-1.1	(S) on average 1.0 1.0
7	EC-Earth3	IFS cy36r4	HTESSEL	(S) 0.703 0.703
8	FGOALS-f3-L	FAMIL2.2	CLM4.0	(S) 1.0 1.0
9	FIO-ESM-2-0	CAM4	CLM4.0	1.25 0.938
10	GFDL-ESM4	GFDL-AM4.1	GFDL-LM4.1	(S) 1.0 1.0
11	INM-CM5-0	INM-AM5-0	INM-LND1	2.0 1.5
12	IPSL-CM6A-LR	LMDZ-NPv6	ORCHIDEE-2.0	2.5 1.268
13	KACE-1-0-G	MetUM-HadGEM3-GA7.1	JULES-HadGEM3-GL7.1	1.25 1.875
14	MIROC6	CCSR AGCM	MATSIRO6.0	(S) 1.406 1.406
15	MPI-ESM1-2-HR	ECHAM6.3	JSBACH3.20	(S) 0.938 0.938
16	MRI-ESM2-0	MRI-AGCM3.5	HAL-1.0	(S) 1.125 1.125
17	NorESM2-LM	CAM-OSLO	CLM	1.875 2.5
18	TaiESM1	TaiAM1	CLM4.0	1.25 0.938

The column “Horizontal resolution” presents the horizontal resolution of the atmosphere module; the spectral atmosphere models are marked with (S) (see also [https://wcrp-cmip.github.io/CMIP6\\_CVs/docs/CMIP6\\_source\\_id.html](https://wcrp-cmip.github.io/CMIP6_CVs/docs/CMIP6_source_id.html)).

Data on the water discharge in the arms of the mentioned rivers (Khabarovsk station for the Amur River and Mostovoi station for the Selenga River corresponding to the catchment areas of  $1.63 \cdot 10^6$  and  $0.36 \cdot 10^6$  km<sup>2</sup>, respectively) from <https://gmvo.skniivh.ru/index.php?id=1> were taken as reference data  $D$  for runoff. The mask of the Amur River catchment was specified according to [29]. The spatial mask of the Selenga River catchment was obtained from O.Yu. Antokhina (private communication). Precipitation over the catchment was determined by the interpolation of model simulations to the general  $0.5 \cdot 0.5$  grid.

The ensemble mean  $E(R|D)$  caused by reference data  $D$  was calculated using the formula

$$E(R|D) = \sum_k R^{(k)} W^{(k)} \quad (1)$$

where  $R^{(k)}$  is the values of runoff for the model with the number  $k$ , summation is carried out by the index  $k$ .

The value of  $E(R|D)$  can be calculated in different ways with different selections of Bayesian weights  $W^{(k)}$ . The simplest method is when the same weight  $W^{(k)} = W_0 = 1/N$  ( $N$  is the number of models in the ensemble; this approach is often called “model democracy” [33, 34]) is attributed to all models. Another approach includes the calculation of weights depending on how well the model reproduces the selected climatic characteristics as compared to real (reference) data. In this,  $W^{(k)}$  is calculated as a likelihood function for each model as compared to reference data  $D$  [36]: this is the approach with the Bayesian averaging [6, 8, 24, 31].

On the interannual scale, river runoff is characterized by the difference between precipitation  $P$  and evaporation in the catchment. Data on precipitation over the catchments were also used to determine the Bayesian weights. The GPCP 2.3 (The Global Precipitation Climatology Project, version 2.3) [23] (pr in the CMIP6 archive) dataset was taken as reference data for precipitation. Reference data for evapotranspiration were not used due to the absence of reliable large-scale data.

The above likelihood functions were considered normally distributed by each variable [6, 8, 24]. In particular, the following characteristics were computed for the variable  $Y$  ( $Y = R, P$ ):

$$w_{Y,i}^{(k)} = \left( Y_i^{(k)} ; Y_i^{(D)}, \sigma_i^{(D)} \right) \quad (2)$$

where  $(y; y^{(D)}, \sigma^{(D)})$  is the normal distribution for the variable  $y$  with the mean value  $y^{(D)}$  and standard deviation  $\sigma^{(D)}$ ; the superscript  $(D)$  indicates the calculation from reference data, the subscript  $i$  is the

characteristic of timescale. Due to the need in analyzing the quality of models on different timescales, the following scores were distinguished:

- the multiyear mean  $Y_m^{(i)}$  ( $i = m$  characterizes the timescale exceeding the length  $I$  of time series, the dot points either to the model number  $k$  or to reference data  $D$ );
- the linear trend coefficient for this variable  $Y_{tr}^{(i)}$  ( $i = tr$  characterizes an interdecadal timescale);
- the standard deviation (SD) of interannual variability  $Y_{IAV}^{(i)}$ , which is determined for the time series  $Y^{(i)}$  after removing the linear trend with the coefficient  $Y_{tr}^{(i)}$  ( $i = IAV$  characterizes an interannual scale) [8].

The value of  $Y_{IAV}^{(i)}$  was used as SD  $Y_i^{(i)}$  for the multiyear mean ( $i = m$ ); for the coefficient of the linear trend ( $i = tr$ ), the root-mean-square estimate of its sample estimation was used; for the interannual SD ( $i = IAV$ ), the value of  $Y_{IAV}^{(i)}$  with  $Y_i = [2/(I - 1)]^{1/4}$  was used. The latter relationship is the estimate of uncertainty for  $Y_{IAV}^{(i)}$  for the time series of finite length  $I$  [44].

Using  $w_{Y,i}^{(k)}$ , the Bayesian weights were determined, in particular:

- the characteristic of the multiyear mean hydrological regime

$$W_m^{(k)} = w_{R,m}^{(k)} w_{P,m}^{(k)}; \tag{3}$$

- the characteristic of the trend coefficient reproduction for runoff and precipitation

$$W_{tr}^{(k)} = w_{R,tr}^{(k)} w_{P,tr}^{(k)}; \tag{4}$$

- the characteristic of reproduction of interannual variability for these variables

$$W_{IAV}^{(k)} = w_{R,IAV}^{(k)} w_{P,IAV}^{(k)}; \tag{5}$$

- the characteristics of reproduction of variations in runoff and precipitation, respectively, on all timescales

$$W_R^{(k)} = w_{R,m}^{(k)} w_{R,tr}^{(k)} w_{R,IAV}^{(k)}; \tag{6}$$

$$W_P^{(k)} = w_{P,m}^{(k)} w_{P,tr}^{(k)} w_{P,IAV}^{(k)}; \tag{7}$$

- the combined weighting factor

$$W_{all}^{(k)} = W_m^{(k)} W_{tr}^{(k)} W_{IAV}^{(k)} W_R^{(k)} W_P^{(k)}. \tag{8}$$

The determination of the Bayesian weights was carried out for the period 1979–2014, which is the common time interval for available data and simulations in the “historical” model experiment (the starting year of the interval is caused by availability of corresponding precipitation data; data on water discharge in the rivers are available since the 1930s). For available model variables, different values of  $N$  correspond to different SSPs (17 for SSP1-2.6, 17 for SSP2-4.5, and 18 for SSP5-8.5). After selecting models for a specific SSP, the weights  $W_j^{(k)}$  ( $j = m, tr, IAV, R, P, all$ ) were normalized:

$$\sum_k W_j^{(k)} = 1. \tag{9}$$

Due to the absence of runoff values for the NorESM2-LM model for the first month under the SSPs for January 2015, the January mean values for the 10 preceding years and 10 next years were used. This should not have an essential effect on the output due to the smallness of the January runoff for the Amur and Selenga river catchments [9, 13, 20].

When selecting the weighting algorithms, there was no aim to find the best algorithm. The objective of the study was to analyze the ensemble statistics depending on the choice of realistic models. In view of this, along with the weights (3)–(8), the arithmetic intermodel mean (that formally corresponds to the averaging with the weights  $W_0$ ) was also used. The results of computing the Bayesian weights are presented in Figs. 1–4.

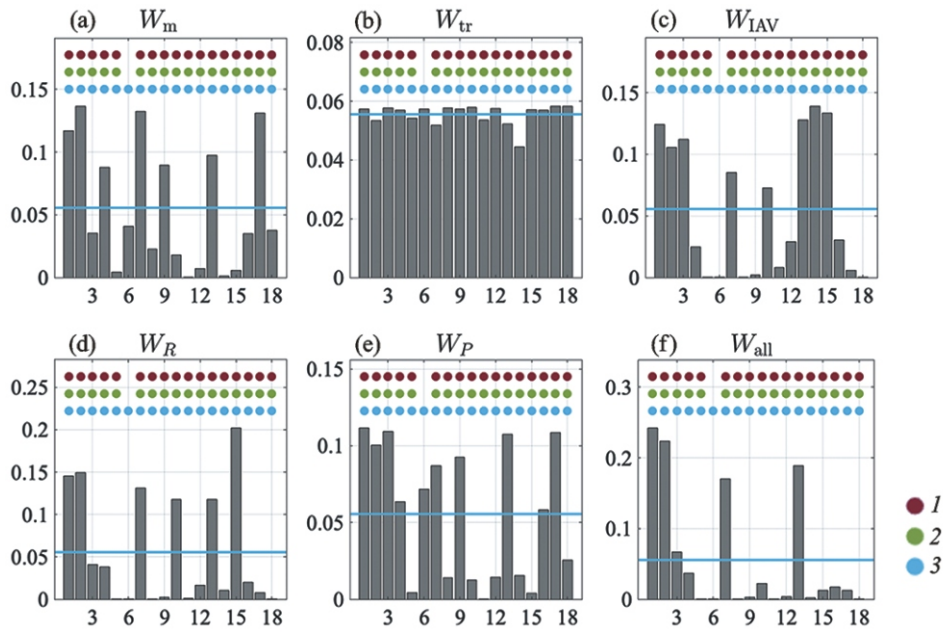


**Fig. 1.** The Bayesian weights for the CMIP6 ensemble models calculated for the Amur basin using the variable *mrrs* (which takes into account only surface runoff): (a)  $W_m$ , (b)  $W_{tr}$ , (c)  $W_{IAV}$ , (d)  $W_R$ , (e)  $W_P$ , and (f)  $W_{all}$  normalized according to the equation (9) for  $N = 18$  (which corresponds to the SSP5-8.5). Here and in Figs. 2, 3, and 4, the model numbers are given on the  $x$ -axis according to Table 1. The horizontal lines are the weights  $W_0$  for the same value of  $N$ . The color circles show which models were used for computing the ensemble statistics for the SSPs: (1) SSP1-2.6; (2) SSP2-4.5; (3) SSP5-8.5.

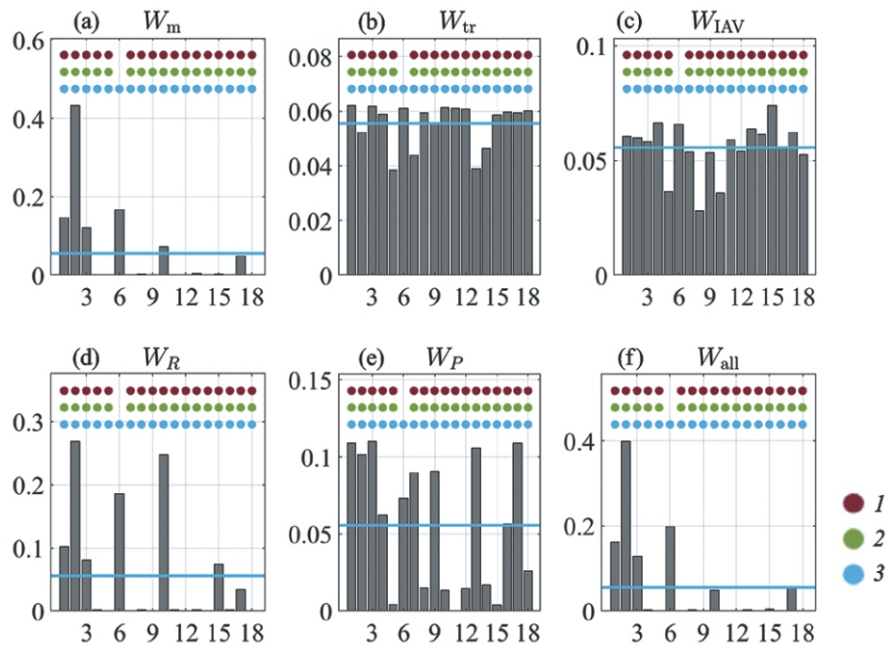


**Fig. 2.** The same as in Fig. 1 using the variable *mrrr* (which takes into account total runoff).

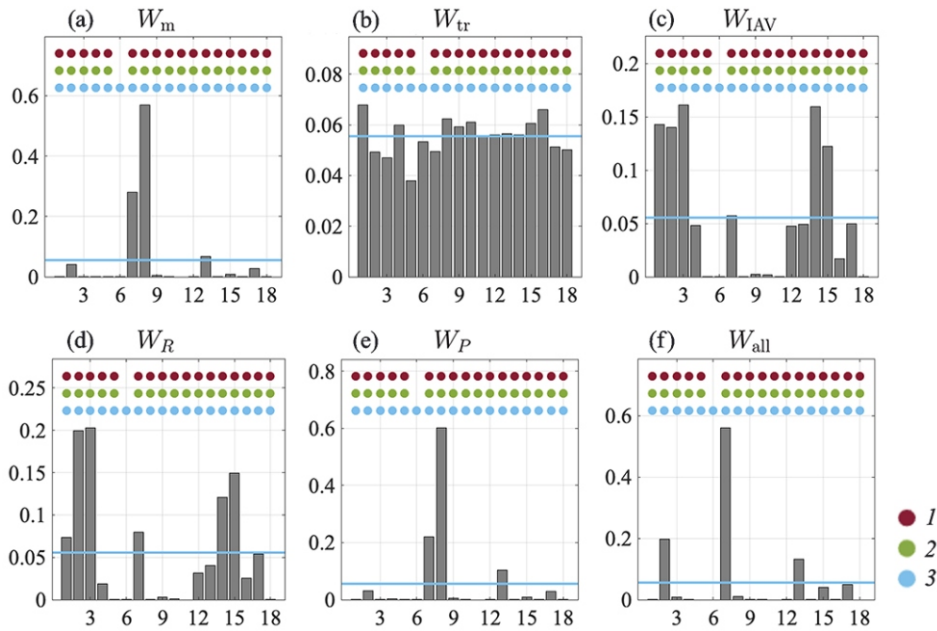


Fig. 3. The same as in Fig. 1 for the Selenga River catchment.

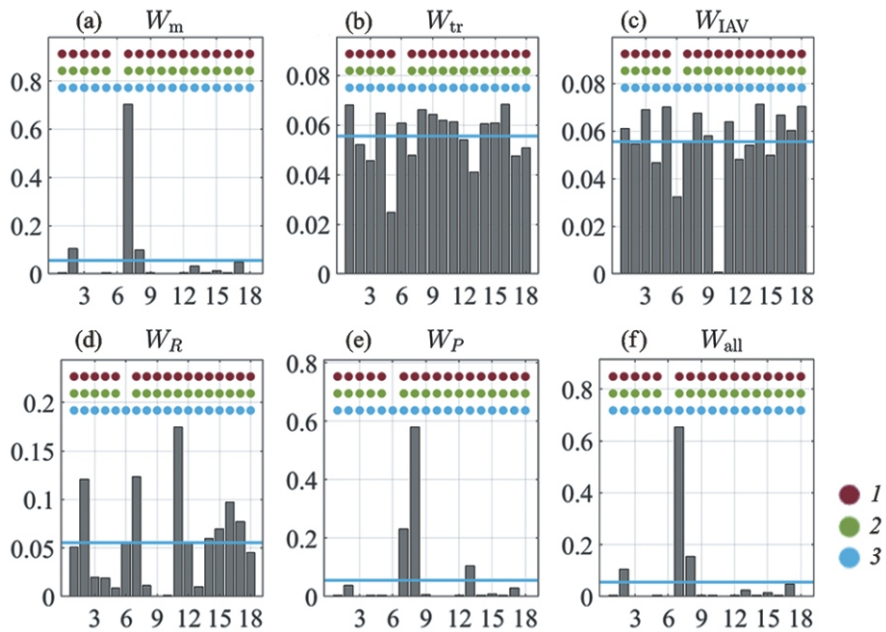


Fig. 4. The same as in Fig. 2 for the Selenga River catchment.

### 3. RESULTS

#### 3.1. Bayesian Weights

For surface runoff (the variable *mrros*, which takes into account surface runoff alone) from the Amur and Selenga catchments, the greatest intermodel differences were found for the multiyear means (the weights  $W_m$ ; hereinafter, for shortness, the model index is not indicated) and interannual SD (the weights  $W_{IAV}$ , Figs. 1 and 3). The intermodel distribution for the trends is more uniform. This is associated with the fact that for 1979–2014, the estimates of the precipitation and runoff trend are statistically indistinguishable from zero both for reference data and for simulations with all models.

For the Selenga River catchment, the intermodel distribution of  $W_m$  is similar to the corresponding distribution of weights for precipitation  $W_P$ , and the intermodal distribution of  $W_{IAV}$  is similar to the distribution of weights for runoff  $W_R$ . At the same time, the intermodel differences in the multiyear mean regime for this catchment are determined mainly by the intermodel differences in precipitation, and the interannual variability is determined by the corresponding variability of runoff. The similar correspondence in the pairs  $W_m-W_P$  and  $W_{IAV}-W_R$  is also manifested for the Amur runoff, although to a smaller extent.

For both catchments, the intermodel distribution of weights for precipitation  $W_P$  is more heterogeneous than for the weights for river runoff  $W_R$ . This indicates that the model deviations for the simulation of precipitation characteristics are compensated by the respective deviations in the simulation of evapotranspiration characteristics, which generally leads to the better simulation of runoff for the CMIP6 ensemble.

For the combined weights  $W_{all}$  characterizing intermodel differences in the simulation of both multiyear means and interannual variability (as well as  $R$  and  $P$ ), there is the most heterogeneous intermodel distribution.

For total runoff (mrro), unlike surface runoff,  $W_{IAV}$  are distributed more uniformly for both catchments (Figs. 2 and 4). For the Amur,  $W_m$  and  $W_{tr}$  are characterized by the significant intermodel differences (see Figs. 1 and 2). The other features of the distribution of weights are similar to those obtained for surface runoff (mrros).

For both analyzed catchments, no significant effect of the horizontal model resolution on the quality of simulation of hydrological cycle characteristics was revealed. No connection was found either between the quality of runoff and precipitation simulation by the models on different timescales and the choice of the atmospheric module of the land active layer in the models (see Table 1). In view of this, it is noteworthy that only 3 of 18 models are characterized by the high value of  $W_{all}$  for both catchments: the EC-Earth (No. 7 in Table 1, with the smallest horizontal size of the model grid (0.7°) and the atmosphere and land modules that are not used in the other models of the ensemble), BCC-CSM2-MR (No. 2 in the table, with the medium horizontal resolution and the atmosphere and land modules that are not used in the other models of the ensemble), and KACE-1-0-G (No. 13 in the table, with the medium horizontal resolution, the atmosphere module from the HadGEM family that is also used in the other models, and the scheme of processes in the land active layer from the JULES family). The models with a low horizontal resolution (INM-CM5-0 and IPSL-CM6A-LR) are generally characterized by relatively small Bayesian weights.

The revealed low correlation of the Bayesian weights with the choice of the model components (atmosphere and land active layer modules) and their horizontal resolution (except for the models with a low horizontal resolution) may be explained by a great contribution of uncertainty related to specifying initial conditions for model simulations for such regional projections on a secular timescale. This differs from the conclusions made in [30, 35], where the analysis was performed not for hydrological variables, but for surface air temperature. It is essential that, unlike surface temperature with a greater trend on a secular scale, the trends in runoff from the Amur and Selenga rivers and in precipitation over their catchments are statistically insignificant with relatively high natural variability (see Section 3.2 below), except for the changes in the Amur total runoff under the SSP5-8.5 with the highest anthropogenic emissions of greenhouse gases to the atmosphere in the 21st century.

High uncertainty of the statistical estimation of Bayesian weights is associated with the high contribution of uncertainty caused by specifying initial condition [46]. Consequently, it is necessary to analyze the ensemble statistics for a different choice of Bayesian weighting schemes (like in the present paper) and to compare the results with the ensemble mean with a uniform distribution of weights among the models (the weights  $W_0$ ) [33].

### 3.2. Ensemble Statistics

#### 3.2.1. The Amur River

For surface runoff (mrros), differences between different types of averaging for the Amur catchment are statistically insignificant: the difference between the Bayesian means for different weights does not exceed 50 km<sup>3</sup>/year, which is comparable with the typical values of the intermodel Bayesian SD [6, 8, 24, 31], which are equal to 60 to 140 km<sup>3</sup>/year depending on the choice of Bayesian weights (not shown). Nevertheless, the intermodel differences between  $E(R|D)$  allow judging about the features of hydrological cycle projections in modern Earth system models.

For the Amur, no statistically significant changes were revealed in  $E(R|D)$  for the 21st century for all types of averaging and the variable that takes into account surface runoff alone (Figs. 5a, 5c, and 5e). At the

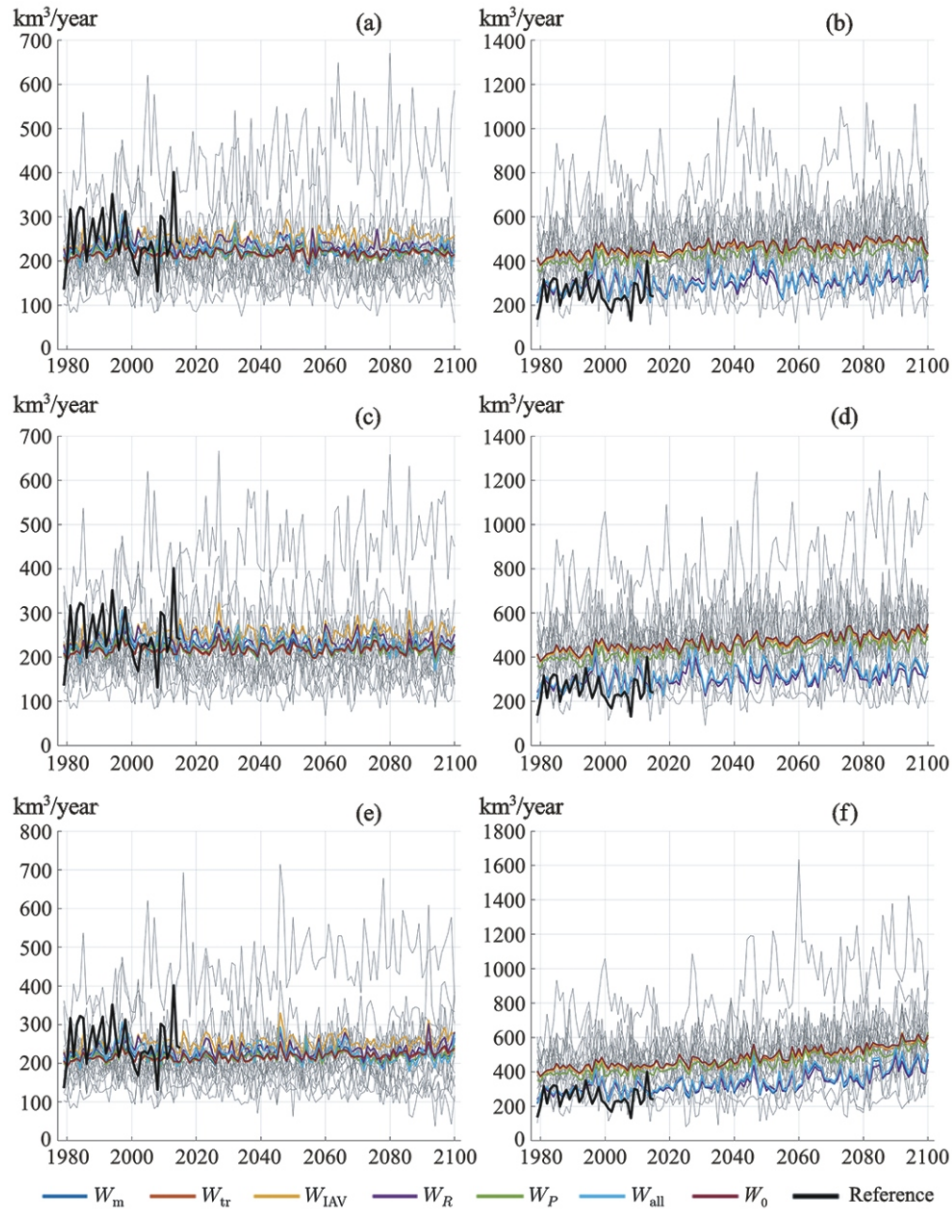


**Fig. 5.** The ensemble means  $E(R|D)$  for annual runoff for the Amur River obtained using different weights for (a, b) the SSP1-2.6, (c, d) SSP2-4.5, and (e, f) SSP5-8.5 scenarios for (a, c, e) the variable mros (which takes into account only surface runoff) and (b, d, f) variable mmro (which takes into account total runoff). Here and in Fig. 7, the thin lines show the results of simulations with individual models.

same time, on average for the model ensemble, there is a general increase in regional precipitation (see [37], Fig. 8.14), which is compensated by a corresponding regional increase in evapotranspiration (see [37], Fig. 8.17).

The ensemble means of annual surface runoff  $R$  in case of using  $W_m$  and  $W_P$  are close. A close to them ensemble mean for runoff was also obtained in case of using  $W_{tr}$  (and  $W_0$ ). The value of  $E(R|D)$  obtained using these weights for the Amur catchment is smaller than for the other weights, especially for  $W_R$  and  $W_{IAV}$ .

For total runoff (mmro), the type of  $E(R|D)$  noticeably changes (Figs. 5b, 5d, and 5f). The Bayesian means obtained using  $W_{tr}$ ,  $W_{IAV}$ ,  $W_P$ , and  $W_0$  are close in the value and are 30–50% higher than the means obtained for the other weights. At the same time, the difference in the values of runoff ( $\sim 100$  km<sup>3</sup>/year) becomes comparable with the value of the intermodel Bayesian SD. Under the SSP5-8.5, there is a positive



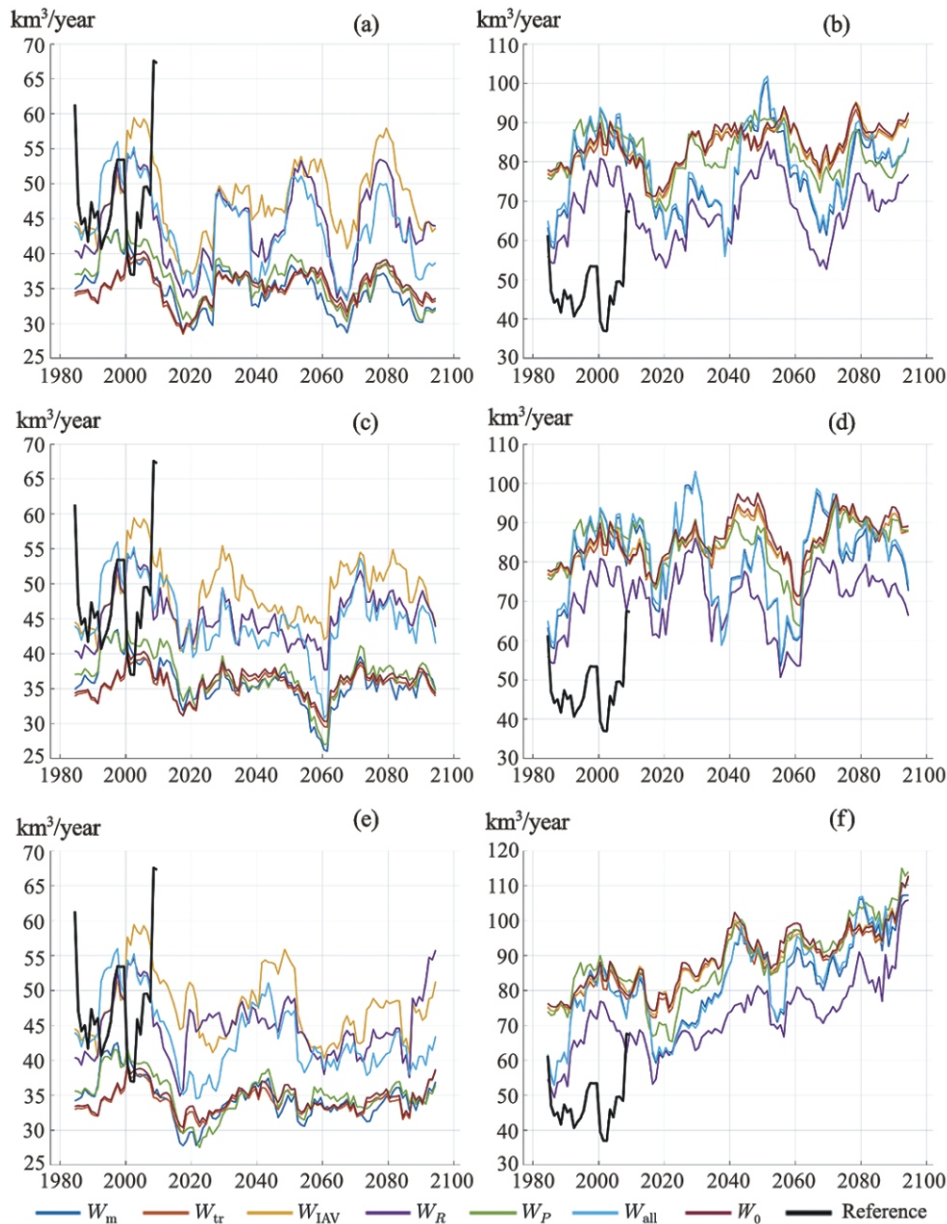


**Fig. 6.** The ensemble means  $E(\sigma_{R, IAV} | D)$  for the standard deviation of annual runoff for the Amur River obtained using different weights for (a, b) the SSP1-2.6, (c, d) SSP2-4.5, and (e, f) SSP5-8.5 scenarios for (a, c, e) the variable mrrros (which takes into account only surface runoff) and (b, d, f) variable mrrro (which takes into account total runoff).

trend of about  $1.7(0.3) \text{ km}^3/\text{year}^2$  (the limits of the 95% confidence interval are given in brackets). According to the results, the use of precipitation data alone when configuring the Earth system models leads to the underestimation of the Amur runoff, and the use of data on river runoff alone leads to the overestimation of precipitation (and, hence, evapotranspiration) in the models. It should be noted that for the “historical” scenario, the models generally overestimate annual precipitation over the Amur catchment.

As already noted, extreme hydrological events are often manifested in the form of either extremely high or extremely low values of runoff in some years. Such events are uncorrelated among the models, which is one of the manifestations of uncertainty related to specifying initial conditions for integration and, hence, disappear in case of ensemble averaging. Their analysis is possible in terms of the ensemble mean  $E(\sigma_{R, IAV} | D)$ . The value of  $\sigma_{R, IAV}$  was calculated for the whole interval of 1979–2014 during the Bayesian weighting, while it was calculated for the moving windows with a length of 11 and 21 years for analyzing

the variability of runoff. In general, the results differ little for such moving windows, therefore, only the results for the 11-year window are presented.

When analyzing surface runoff (mmros), as well as for  $E(R|D)$ , no statistically significant linear trends in the Bayesian ensemble mean for  $\sigma_{R, IAV}$  were revealed (Figs. 6a, 6c, and 6e). At the same time, the periods of high and low variability are manifested, with a variation range for  $\sigma_{R, IAV}$  between the maximum and minimum values of about 1/3 of the mean. The highest absolute value of  $E(\sigma_{R, IAV}|D)$  is reached at the beginning of the 21st century. The resulting variations are statistically insignificant: for the 11-year window ( $I = 11$ ), even not taking into account the autocorrelation of time series, relative uncertainty of the SD estimation is  $\approx 0.67$  (see Section 2). The uncertainty in the model projections of future changes in the Earth system state associated with specifying initial conditions for numerical simulations hampers the interpretation of the results with referencing to specific time intervals (this is not valid for the period of 1979–2014, for which the timing is carried out implicitly by calculating the Bayesian weights). At the same time, significant variations in the characteristics of interannual variability of the Amur runoff were revealed in the 21st century (with relatively small trends in the mean runoff). The noted variations in the SD of interannual variability of the Amur runoff are close to quasiperiodic, with a variation period of about 20 years. The range of such quasiperiodic variations in  $E(\sigma_{R, IAV}|D)$  generally decreases as climate warms. The more considerable the warming is, the greater this decrease is (Figs. 6c and 6e), although this result is not statistically significant.

For total runoff (Figs. 6b, 6d, and 6f), the values of the mean  $E(\sigma_{R, IAV}|D)$  are higher than for surface runoff by about two times. Under the SSP5-8.5 (Fig. 6f), a small positive trend emerges, which is not statistically significant though. Other features revealed for surface runoff (mmros) are also manifested for total runoff.

### 3.2.2. The Selenga River

Some results obtained for the Selenga River are generally similar to the results for the Amur River. In particular, for the Selenga River, no statistically significant trends were revealed for  $E(R|D)$  (Fig. 7) and  $E(\sigma_{R, IAV}|D)$  (Fig. 8) without and with consideration of groundwater runoff.

It was found for surface runoff that the Bayesian means for river runoff in case of using  $W_{IAV}$  and  $W_R$  differ little and are noticeably greater (by about 1/3) than those obtained for  $W_m$ ,  $W_P$ , and  $W_{all}$  (which, in turn, also lead to the close values of  $E(R|D)$ ). This, in particular, indicates a general underestimation of the Selenga River runoff in the models. The Bayesian means in case of using  $W_{tr}$  are between those for  $W_{IAV}$  and  $W_R$  on the one hand and  $W_m$ ,  $W_P$ , and  $W_{all}$  on the other hand. This averaging is also close to the averaging with equal weights for all models due to an almost uniform intermodel distribution of  $W_{tr}$ .

For total runoff, the Bayesian means in case of using  $W_P$ ,  $W_{tr}$ , and  $W_{IAV}$  are close in the value and are about a third higher than those obtained with  $W_m$ ,  $W_R$ , and  $W_{all}$ , which are also close to each other. The means with  $W_m$ ,  $W_P$ ,  $W_{all}$ , and  $W_0$  overestimate the value of the Selenga River runoff as compared to observational data. By the end of the 21st century under the SSP5-8.5, there is a small and statistically insignificant positive trend.

The conclusion made for the Amur catchment about the results of estimating the relative significance of the models in the ensemble in terms of the quality of data simulation for different variables ( $R$  or  $P$ ) by them is also valid for the Selenga River catchment.

For surface runoff of the Selenga River, as well as for the Amur, in case of the averaging leading to the higher  $R$ ,  $\sigma_{R, IAV}$  is also higher (Figs. 8a, 8c, and 8e). The ensemble means  $E(\sigma_{R, IAV}|D)$  with the weights  $W_{IAV}$ ,  $W_R$ , and  $W_{all}$  are consistent with observations for 1979–2014, whereas the corresponding averaging with the other weights (including  $W_0$ ) underestimates the empirical value of  $\sigma_{R, IAV}$  by a fourth or a third.

A distinctive feature of the Selenga River catchment as compared with the Amur catchment is less pronounced variations in  $\sigma_{R, IAV}$  (Figs. 8a, 8c, and 8e) without quasiperiodic variability. At the same time, the periods of high and low variability are manifested, with a range between the maximum and minimum values of  $\sigma_{R, IAV}$  that is about 1/6 of the mean value.

For all SSPs used in the present study, the period of available observations is followed by the period of low values of  $E(\sigma_{R, IAV}|D)$ , with a subsequent noticeable increase in the second half of the 21st century. This increase is especially long and significant in absolute value for the averaging with  $W_{IAV}$  and  $W_R$  and makes up about 1/3 of the mean value.

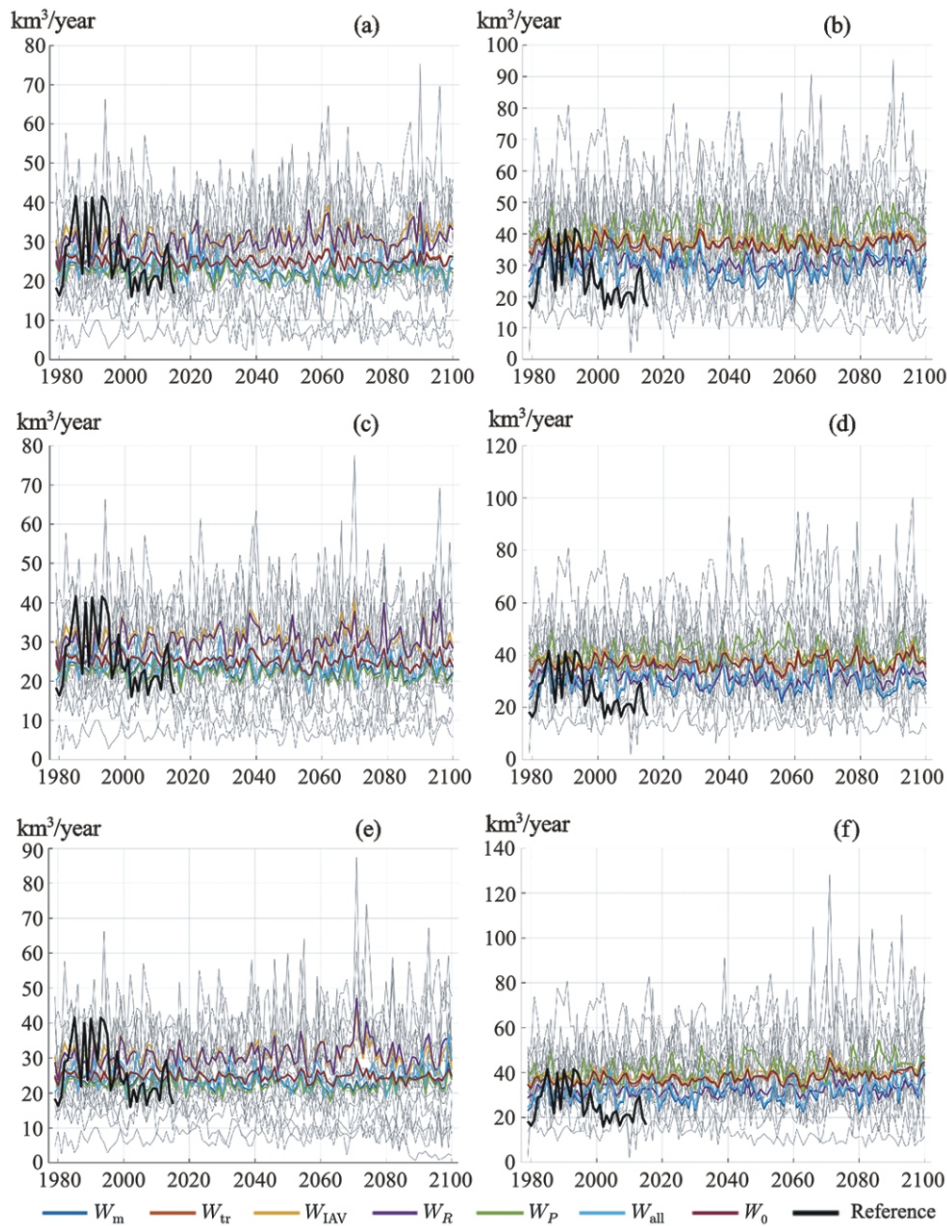


Fig. 7. The same as in Fig. 5 for the Selenga River.

For total runoff of the Selenga River (Figs. 8b, 8d, and 8f), the ensemble means  $E(\left. R, IAV \right| D)$  for all weights have close values, which are consistent with observations. As well as for the Amur runoff, the total runoff of the Selenga River is characterized by quasiperiodic variations, which have the smallest relative range but similar periods of variability. No significant trends were revealed either.

#### 4. CONCLUSIONS

The changes in runoff of the Amur and Selenga rivers in the 21st century were analyzed using the ensemble of the CMIP6 climate models and the Bayesian weighting. The choice of the Bayesian weights was determined by the quality of the model simulation of river runoff and precipitation over the catchments on different timescales. In particular, multiyear means, linear trends, and interannual variability characterized by standard deviations were analyzed. Data from the stream gages (Khabarovsk for the Amur River and Mostovoi for the Selenga River) for annual runoff and GPCP-2.3 dataset for annual precipitation over the catchments were used as reference data for the Bayesian weighting.

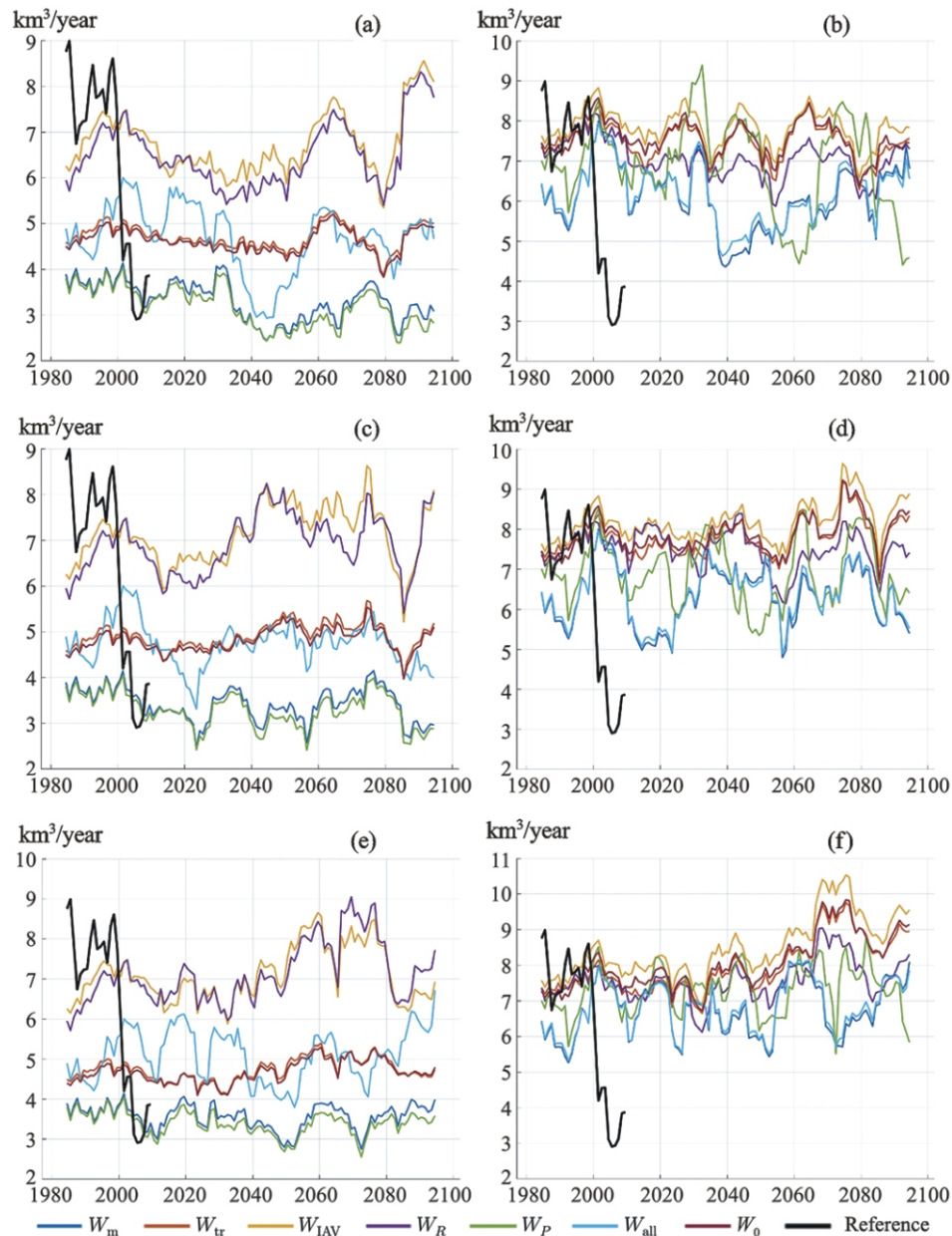


Fig. 8. The same as in Fig. 6 for the Selenga River.

For the Amur and Selenga catchments, the greatest intermodel differences were found for the weights  $W_m$  and  $W_{IAV}$ , which characterize the multiyear mean runoff and SD of interannual variability, respectively. At the same time, the intermodel distribution of weights  $W_m$  was found to be similar to the corresponding distribution for precipitation  $W_P$ , and the intermodel distribution of  $W_{IAV}$  was similar to the distribution of weights for runoff  $W_R$ . For the Selenga River, this correspondence is more clearly pronounced than for the Amur River. For both catchments, no significant effect of horizontal resolution of the model with the selection of the atmosphere module or the land active layer module on the values of Bayesian weights was found. For total runoff in the Amur basin, the averaging with all weights revealed a positive trend in the 21st century for all analyzed scenarios of anthropogenic forcing. No similar trend was revealed for total runoff of the Selenga River.

The results obtained for the Amur River can be compared with the results of [4], where the prevalence of the negative runoff anomalies was found for all SSPs in the 21st century both for the climate models of the previous generation (CMIP5) and for the hydrological model in case of specifying atmospheric forcing

based on the ensemble means for the CMIP5 ensemble models. The difference in the results of the present study, on the one hand, and paper [4], on the other hand, may be associated with corresponding differences in the algorithms for the calculation of ensemble statistics. In particular, even not taking into account differences between different generations of the models, it may be noted that only three of nine models used in [4] are characterized by a significant contribution to the Bayesian means in the present paper (Fig. 2). This additionally highlights the usefulness and need in the analysis of different assumptions about the algorithms for assessing the quality of Earth system models when evaluating future climate change.

For surface runoff in both catchments, no statistically significant changes were revealed in annual runoff and SD of its interannual variability (on a timescale up to decadal one) for the 21st century as a whole for all types of averaging applied. At the same time, the interdecadal variations in the SD of interannual variability were found: up to 1/3 of the multiyear mean  $\sigma_{R, IAV}$  for the corresponding catchment. For the Amur, the variations in the SD of interannual variability for runoff are close to quasiperiodic, with a variation period of about two decades. For total runoff, the SD of interannual variability is higher by about two times, similar variations are observed for the Selenga River. In [14], the connection of such cyclicity of the Amur runoff with the Pacific Decadal Oscillation was noted.

The low correlation of the Bayesian weights with the horizontal resolution of climate models and the choice of the atmosphere module or the land surface module in the models may be explained by the large contribution of uncertainty related to initial conditions for such regional projections on a secular timescale with a relatively small secular variation in runoff. This is possible for a small secular trend in the corresponding variable and for the high SD of interannual variability. The noted uncertainty hampers the referencing of the revealed periods of high and low interannual variability of river runoff to the specific time intervals. The detailed timing of such events for modern models is feasible only in the framework of decadal projections [26, 38].

#### ACKNOWLEDGMENTS

The authors thank O.Yu. Antokhina for presenting the data of the Selenga River catchment mask and A.N. Gelfan for constructive comments to the earlier version of the paper.

#### FUNDING

The analysis of runoff variations depending on timescales and the estimation of variability of regional runoff due to global climate change was supported by the Russian Science Foundation (grants 21-17-00021 and 19-17-00240, respectively). The features of the modern variability of hydrological regime in the regions of Northern Eurasia were analyzed in the framework of Agreement No. 075-15-2020-776 with the Ministry of Science and Higher Education of the Russian Federation. A part of the study was carried out in the framework of the Governmental Assignment of Shirshov Institute of Oceanology of Russian Academy of Sciences (theme 0128-2021-0010).

#### REFERENCES

1. M. M. Arzhanov, A. V. Eliseev, P. F. Demchenko, I. I. Mokhov, and V. Ch. Khon, "Simulation of Thermal and Hydrological Regimes of Siberian River Watersheds under Permafrost Conditions from Reanalysis Data," *Izv. Akad. Nauk, Fiz. Atmos. Okeana*, No. 1, **44** (2008) [*Izv., Atmos. Oceanic Phys.*, No. 1, **44** (2008)].
2. K. Arpe, L. Bengtsson, G. S. Golitsyn, I. I. Mokhov, V. A. Semenov, and P. V. Sporyshev, "Analysis and Modeling of the Hydrological Regime Variations in the Caspian Sea Basin," *Dokl. Akad. Nauk*, No. 2, **366** (1999) [*Dokl. Earth Sci.*, No. 4, **366** (1999)].
3. K. Arpe, L. Bengtsson, G. S. Golitsyn, L. K. Efimova, I. I. Mokhov, V. A. Semenov, and V. Ch. Khon, "Variations in a Hydrological Cycle at the Lake Ladoga Catchment and the Neva Runoff in the 20th and 21st Centuries as Analyzed by a Global Climate Model," *Meteorol. Gidrol.*, No. 12 (2000) [*Russ. Meteorol. Hydrol.*, No. 12 (2000)].
4. A. N. Gelfan, A. S. Kalugin, and Yu. G. Motovilov, "Assessing Amur Water Regime Variations in the XXI Century with Two Methods Used to Specify Climate Projections in River Runoff Formation Model," *Vodnye Resursy*, No. 3, **45** (2018) [*Water Resour.*, No. 3, **45** (2018)].
5. A. V. Eliseev, M. M. Arzhanov, P. F. Demchenko, and I. I. Mokhov, "Changes in Climatic Characteristics of Northern Hemisphere Extratropical Land in the 21st Century: Assessments with the IAP RAS Climate Model," *Izv. Akad. Nauk, Fiz. Atmos. Okeana*, No. 3, **45** (2009) [*Izv., Atmos. Oceanic Phys.*, No. 3, **45** (2009)].

6. A. V. Eliseev and V. A. Semenov, "Arctic Climate Changes in the 21st Century: Ensemble Model Estimates Accounting for Realism in Present-day Climate Simulation," *Dokl. Akad. Nauk*, No. 2, **471** (2016) [*Dokl. Earth Sci.*, No. 1, **471** (2016)].
7. I. L. Kalyuzhnyi and S. A. Lavrov, "Basic Physical Processes and Regularities of Winter and Spring River Runoff Formation under Climate Warming Conditions," *Meteorol. Gidrol.*, No. 1 (2012) [*Russ. Meteorol. Hydrol.*, No. 1, **37** (2012)].
8. O. V. Kibanova, A. V. Eliseev, I. I. Mokhov, and V. Ch. Khon, "Variations in the Duration of the Navigation Period along the Northern Sea Route in the 21st Century Based on Simulations with an Ensemble of Climatic Models: Bayesian Estimates," *Dokl. Akad. Nauk*, No. 1, **481** (2018) [*Dokl. Earth Sci.*, No. 1, **481** (2018)].
9. O. Yu. Marchenko, V. I. Mordvinov, and T. V. Bereznykh, "Extreme Water Content of the Selenga River and Summertime Atmospheric Circulation Features," *Meteorol. Gidrol.*, No. 10 (2012) [in Russian].
10. V. P. Meleshko, G. S. Golitsyn, E. M. Volodin, V. Ya. Galin, V. A. Govorkova, A. V. Meshcherskaya, I. I. Mokhov, T. V. Pavlova, and P. V. Sporyshev, "Calculation of Water Balance Components over the Caspian Sea Watershed with a Set of Atmospheric General Circulation Models," *Izv. Akad. Nauk, Fiz. Atmos. Okeana*, No. 4, **34** (1998) [*Izv., Atmos. Oceanic Phys.*, No. 4, **34** (1998)].
11. V. P. Meleshko, V. A. Govorkova, V. M. Kattsov, S. P. Malevskii-Malevich, E. D. Nadezhina, P. V. Sporyshev, G. S. Golitsyn, P. F. Demchenko, A. V. Eliseev, I. I. Mokhov, V. A. Semenov, and V. C. Khon, "Anthropogenic Climate Change in Russia in the Twenty-First Century: An Ensemble of Climate Model Projections," *Meteorol. Gidrol.*, No. 4 (2004) [*Russ. Meteorol. Hydrol.*, No. 4 (2004)].
12. V. M. Moreido and A. S. Kalugin, "Assessing Possible Changes in Selenga R. Water Regime in the XXI Century Based on a Runoff Formation Model," *Vodnye Resursy*, No. 3, **44** (2017) [*Water Resour.*, No. 3, **44** (2017)].
13. I. I. Mokhov, "Hydrological Anomalies and Tendencies of Change in the Basin of the Amur River under Global Warming," *Dokl. Akad. Nauk*, No. 5, **455** (2014) [*Dokl. Earth Sci.*, No. 2, **455** (2014)].
14. I. I. Mokhov, "Extreme Atmospheric and Hydrological Phenomena in Russian Regions: Relationship with the Pacific Decadal Oscillation," *Dokl. Akad. Nauk*, No. 2, **500** (2021) [*Dokl. Earth Sci.*, No. 2, **500** (2021)].
15. I. I. Mokhov, P. F. Demchenko, A. V. Eliseev, V. Ch. Khon, and D. V. Khvorost'yanov, "Estimation of Global and Regional Climate Changes during the 19th–21st Centuries on the Basis of the IAP RAS Model with Consideration for Anthropogenic Forcing," *Izv. Akad. Nauk, Fiz. Atmos. Okeana*, No. 5, **38** (2002) [*Izv., Atmos. Oceanic Phys.*, No. 5, **38** (2002)].
16. I. I. Mokhov, A. V. Eliseev, P. F. Demchenko, V. Ch. Khon, M. G. Akperov, M. M. Arzhanov, A. A. Karpenko, V. A. Tikhonov, A. V. Chernokulsky, and E. V. Sigaeva, "Climate Changes and Their Assessment Based on the IAP RAS Global Model Simulations," *Dokl. Akad. Nauk*, No. 2, **402** (2005) [*Dokl. Earth Sci.*, No. 4, **402** (2005)].
17. I. I. Mokhov and V. Ch. Khon, "Hydrological Regime in Siberian River Basins: Model Estimates of Changes in the 21st Century," *Meteorol. Gidrol.*, No. 8 (2002) [*Russ. Meteorol. Hydrol.*, No. 8 (2002)].
18. I. I. Mokhov, V. Ch. Khon, A. V. Timazhev, A. V. Chernokulsky, and V. A. Semenov, "Hydrological Anomalies and Trends in the Amur River Basin due to Climate Change," in *Extreme Floods in the Amur River Basin: Causes, Forecasts, Recommendations* (Roshydromet, Moscow, 2014) [in Russian].
19. N. N. Romanovskii, S. N. Buldovich, G. S. Tipenko, D. O. Sergeev, M. V. Kasymkaya, and A. V. Gavrilov, "Estimation of the Influence of Climate Changes on Surface Runoff by Simulation of Thermal Interaction between Groundwater and Permafrost: A Case Study for the Upper Lena Watershed," *Kriosfera Zemli*, No. 1, **13** (2009) [in Russian].
20. N. L. Frolova, P. A. Belyakova, V. Yu. Grigor'ev, A. A. Sazonov, and L. V. Zotov, "Many-year Variations of River Runoff in the Selenga Basin," *Vodnye Resursy*, No. 3, **44** (2017) [*Water Resour.*, No. 3, **44** (2017)].
21. V. Ch. Khon and I. I. Mokhov, "The Hydrological Regime of Large River Basins in Northern Eurasia in the XX–XXI Centuries," *Vodnye Resursy*, No. 1, **39** (2012) [*Water Resour.*, No. 1, **39** (2012)].
22. I. A. Shiklomanov, V. Yu. Georgievskii, A. L. Shalygin, et al., "Prognostic Assessments of Runoff Changes Based on Climate Scenarios," in *Water Resources of Russia and Their Use* (GGI, St. Petersburg, 2008) [in Russian].
23. R. F. Adler, M. R. P. Sapiano, G. J. Huffman, J. Wang, G. Gu, D. Bolvin, L. J. V. Chiu, U. Schneider, A. Becker, E. Nelkin, P. Xie, R. Ferraro, and D.-B. Shin, "The Global Precipitation Climatology Project (GPCP) Monthly Analysis (New Version 2.3) and a Review of 2017 Global Precipitation," *Atmosphere*, No. 4, **9** (2018).
24. M. M. Arzhanov, A. V. Eliseev, and I. I. Mokhov, "A Global Climate Model Based Bayesian Climate Projection for Northern Extra-tropical Land Areas," *Glob. Planet. Change*, **86–87** (2012).
25. S. Berezovskaya, D. Yang, and D. L. Kane, "Compatibility Analysis of Precipitation and Runoff Trends over the Large Siberian Watersheds," *Geophys. Res. Lett.*, No. 21, **31** (2004).
26. G. J. Boer, D. M. Smith, C. Cassou, F. Doblas-Reyes, G. Danabasoglu, B. Kirtman, Y. Kushnir, M. Kimoto, G. Meehl, R. Msadek, W. Mueller, K. Taylor, F. Zwiers, M. Rixen, Y. Ruprich-Robert, and R. Eade, "The Decadal Climate Prediction Project (DCPP) Contribution to CMIP6," *Geosci. Model Devel.*, No. 10, **9** (2016).
27. A. Dai and K. E. Trenberth, "Estimates of Freshwater Discharge from Continents: Latitudinal and Seasonal Variations," *J. Hydrology*, No. 12, **3** (2002).

28. D. Gerten, S. Rost, W. von Bloh, and W. Lucht, "Causes of Change in 20th Century Global River Discharge," *Geophys. Res. Lett.*, No. 20, **35** (2004).
29. S. T. Graham, J. S. Famiglietti, and D. R. Maidment, "Five-minute, 1/2 , and 1 Data Sets of Continental Watersheds and River Networks for Use in Regional and Global Hydrologic and Climate System Modeling Studies," *Water Resour. Res.*, No. 2, **35** (1999).
30. E. Hawkins and R. Sutton, "The Potential to Narrow Uncertainty in Regional Climate Predictions," *Bull. Amer. Meteorol. Soc.*, No. 8, **90** (2009).
31. J. A. Hoeting, D. Madigan, A. E. Raftery, and C. Volinsky, "Bayesian Model Averaging: A Tutorial," *Stat. Sci.*, No. 4, **14** (1999).
32. V. M. Kattsov, J. E. Walsh, W. L. Chapman, V. A. Govorkova, T. Pavlova, and X. Zhang, "Simulation and Projection of Arctic Freshwater Budget Components by the IPCC AR4 Global Climate Models," *J. Hydrology*, No. 3, **8** (2007).
33. R. Knutti, "The End of Model Democracy?," *Climate Change*, No. 3–4, **102** (2010).
34. R. Knutti, J. Sedlacek, B. M. Sanderson, R. Lorenz, E. Fischer, and V. Eyring, "A Climate Model Projection Weighting Scheme Accounting for Performance and Interdependence," *Geophys. Res. Lett.*, No. 4, **44** (2017).
35. F. Lehner, C. Deser, N. Maher, J. Marotzke, E. Fischer, L. Brunner, R. Knutti, and E. Hawkins, "Partitioning Climate Projection Uncertainty with Multiple Large Ensembles and CMIP5/6," *Earth Syst. Dyn.*, No. 2, **11** (2020).
36. S. S. Leroy, "Detecting Climate Signals: Some Bayesian Aspects," *J. Climate*, No. 4, **11** (1998).
37. V. Masson-Delmotte, P. Zhai, A. Pirani, S. L. Connors, C. Pean, S. Berger, N. Caud, Y. Chen, L. Goldfarb, M. I. Gomis, M. Huang, K. Leitzell, E. Lonnoy, J. B. R. Matthews, T. K. Maycock, T. Waterfield, O. Yelekci, R. Yu, and B. Zhou, *Climate Change 2021: The Physical Science Basis. Contribution of Working Group I to the Sixth Assessment Report of the Intergovernmental Panel on Climate Change* (Cambridge Univ. Press) [in press].
38. G. A. Meehl, L. Goddard, G. Boer, R. Burgman, G. Branstator, C. Cassou, S. Corti, G. Danabasoglu, F. Doblas-Reyes, E. Hawkins, A. Karspeck, M. Kimoto, A. Kumar, D. Matei, J. Mignot, R. Msadek, A. Navarra, H. Pohlmann, M. Rienecker, T. Rosati, E. Schneider, Doug M. Smith, R. Sutton, H. Teng, G. V. Oldenborgh, G. Vecchi, and S. Yeager, "Decadal Climate Prediction: An Update from the Trenches," *Bull. Amer. Meteorol. Soc.*, No. 2, **95** (2014).
39. J. D. Milliman, K. L. Farnsworth, P. D. Jones, Kehui Xu, and L. Smith, "Climatic and Anthropogenic Factors Affecting River Discharge to the Global Ocean, 1951–2000," *Glob. Planet. Change*, No. 3–4, **62** (2008).
40. I. I. Mokhov and M. R. Parfenova, "Changes of the Selenga River Runoff in the Lake Baikal Basin and Their Relationship to El Niño Phenomena," in *Research Activities in Atmospheric and Oceanic Modelling*, Ed. by E. Astakhova, Rep. No. 49, WCRP Rep. No. 12, S. 2 (2019).
41. T. F. Stocker, D. Qin, G.-K. Plattner, L. V. Alexander, S. K. Allen, N. L. Bindoff, F.-M. Breon, J. A. Church, U. Cubasch, S. Emori, P. Forster, P. Friedlingstein, N. Gillett, J. M. Gregory, D. L. Hartmann, E. Jansen, B. Kirtman, R. Knutti, K. Krishna Kumar, P. Lemke, J. Marotzke, V. Masson-Delmotte, G. A. Meehl, I. I. Mokhov, S. Piao, V. Ramaswamy, D. Randall, M. Rhein, M. Rojas, C. Sabine, D. Shindell, L. D. Talley, D. G. Vaughan, and S.-P. Xie, *Climate Change 2013: The Physical Science Basis. Contribution of Working Group I to the Fifth Assessment Report of the Intergovernmental Panel on Climate Change* (Cambridge Univ. Press, Cambridge, United Kingdom and New York, NY, USA, 2013).
42. Q. Tang and D. P. Lettenmaier, "21st Century Runoff Sensitivities of Major Global River Basins," *Geophys. Res. Lett.*, No. 6, **39** (2012).
43. C. Tebaldi and R. Knutti, "The Use of the Multi-model Ensemble in Probabilistic Climate Projections," *Phil. Trans. Roy. Soc. A*, No. 1857, **364** (2007).
44. H. von Storch and F. W. Zwiers, *Statistical Analysis in Climate Research* (Cambridge Univ. Press., Cambridge, 2003).
45. L. Warszawski, K. Frieler, V. Huber, F. Piontek, O. Serdeczny, and J. Schewe, "The Inter-sectoral Impact Model Intercomparison Project (ISI-MIP): Project Framework," *Proc. Nat. Acad. Sci.*, **111** (2014).
46. A. P. Weigel, R. Knutti, M. A. Liniger, and C. Appenzeller, "Risks of Model-weighting in Multimodel Climate Projections," *J. Climate*, No. 15, **23** (2010).
47. H. Yang, F. Zhou, S. Piao, M. Huang, A. Chen, P. Ciaia, Y. Li, X. Lian, S. Peng, and Z. Zeng, "Regional Patterns of Future Runoff Changes from Earth System Models Constrained by Observation," *Geophys. Res. Lett.*, No. 11, **44** (2017).
48. J. Yin, P. Gentile, S. Zhou, S. Sullivan, R. Wang, Y. Zhang, and S. Guo, "Large Increase in Global Storm Runoff Extremes Driven by Climate and Anthropogenic Changes," *Nature Commun.*, No. 1, **9** (2018).
49. X. Zhang, Q. Tang, X. Zhang, and D. P. Lettenmaier, "Runoff Sensitivity to Global Mean Temperature Change in the CMIP5 Models," *Geophys. Res. Lett.*, No. 15, **41** (2014).